Renewable and Sustainable Energy Reviews 16 (2012) 6668–6677

Contents lists available at SciVerse ScienceDirect

Renewable and Sustainable Energy Reviews

journal homepage: www.elsevier.com/locate/rser

Status and potentials of tidal in-stream energy resources in the southern coasts of Iran: A case study

Ali Rashid

Rajaee Teacher Training Center, Department of Fars Province Education, Teachers University, Shiraz, Iran

ARTICLE INFO

Article history:
Received 10 November 2011
Received in revised form
9 August 2012
Accepted 18 August 2012
Available online 5 October 2012

Keywords:
Tidal in-stream energy
Statistical method
Iran
Khowr-e Musa
Tourism

ABSTRACT

Interest in renewable energy in Iran has increased continually over the past decade. Iran has an excellent hydro power energy resource and the use of this resource will assist in the development of a sustainable energy future. Iran – with its many narrow channels and significant tidal range – might be expected to have considerable potential for tidal current power generation. The Khowr-e Musa Bay is a large coastal embayment on the south-western coast of Iran in which the peak tidal currents exceed 2 m/s. It is therefore a promising site for tidal stream power. The assessment employed a statistical method, for estimating tidal current energy resource at the selected site, during one lunar month (since 6 November 1996 to 7 December 1996). With the introduction of constraints and limitations, the technical, practical, accessible and viable tidal current energy resources were obtained.

Contents

1. Introduction . . . 6668
 1.1. Iran power generation and demand . . . 6668
 1.2. Iran and hydro power energy . . . 6670
 1.3. Tides around Iran . . . 6670
2. Tidal energy resource data . . . 6670
3. Tidal stream energy conversion methodology . . . 6670
4. Tidal stream resource methodology . . . 6670
 4.1. Extrapolation of velocity time history to a different channel section . . . 6671
 4.2. Quantification of the tidal stream resource . . . 6672
5. Tidal stream power production methodology . . . 6673
 5.1. Optimal number of turbines . . . 6674
 5.2. Turbine distribution in the farm . . . 6675
6. Compatibility and impacts on recreation and tourism . . . 6675
7. Conclusions . . . 6675
Acknowledgments . . . 6677
References . . . 6677

1. Introduction

1.1. Iran power generation and demand

Iranian energy sector largely depends on the crude oil and natural gas. Due to decreasing fossil fuel resources, the government has decided to control and reduce the energy consumption especially by residential and commercial sectors. The usage of other types of energy specially renewable energy has received great attention from Iran government in recent years [1]. Iran with a population of 73 millions and area of 1,648,000 km^2 is capable of annually (2008) generating 3 MW h electricity per head with an average annual growth of around 6%. The numbers of operative thermal, gas, combined cycle and hydro power generating stations in Iran, based on 2008 data, are 19, 32, 12 and 42 respectively with a

E-mail addresses: Ali.Rashid@farsedu.ir, a.rashid@sci.ui.ac.ir

1364-0321/$ - see front matter © 2012 Elsevier Ltd. All rights reserved.
http://dx.doi.org/10.1016/j.rser.2012.08.010

total installed capacity of 53 GW. Considering the target of 8% economical growth and simultaneously an annual growth of 8% in electric demand, the electric power required in 2025 is expected to reach as high as 195 GW. In that case if the purposed share of electric power to be derived from environmental friendly energy resources is not actualized then more than 80% of the above electric power would be generated by conventional energy resources and mainly by combined cycle power plants [3].

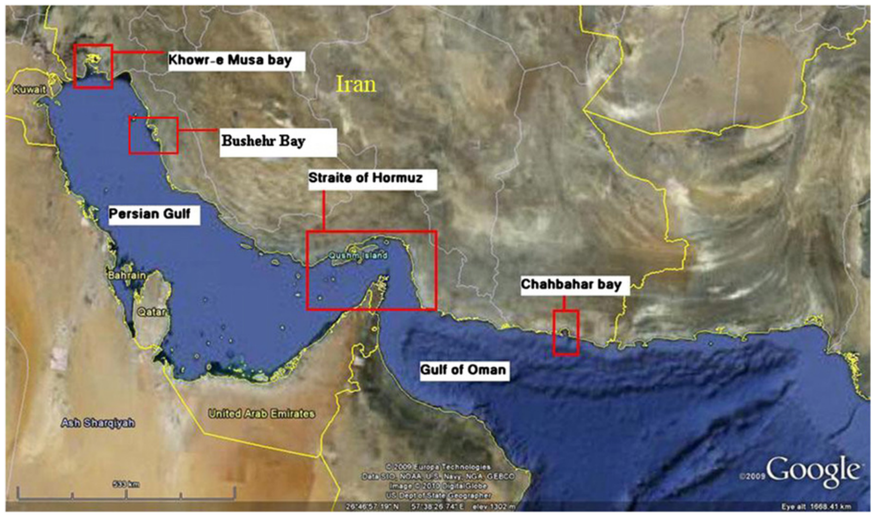


Fig. 1. Study area [2].

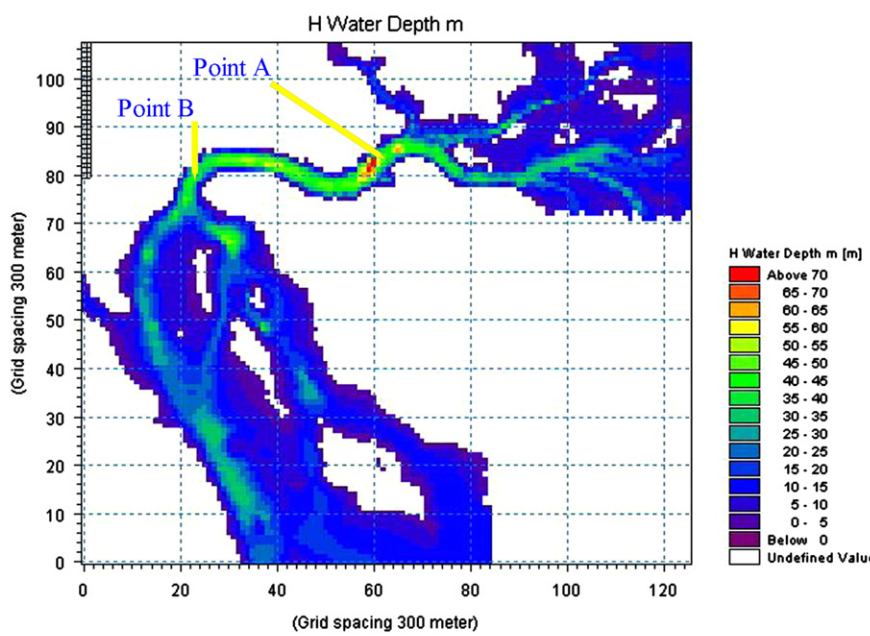


Fig. 2. Khowr-e Musa digital bathymetry.

Area	Peak velocity (m/s)	Adequate water depth for tidal current turbine installation	Not a major shipping lane	Near to the electricity grid	Data available?	Max power density (kW/m^2)
Khowr-e Musa Bay	≤ 2.42	+	-	+	E,V	7.25
Qeshm canal[6]	≤ 1.8	+	-	+	E,V	3
Chahbahar Bay	≤ 0.5	+	-	+	E,V	Negligible
Bushehr Bay	< 0.5	+	-	+	E,V	Negligible

Fig. 3. Potential sites for tidal current power schemes in Iran (E=elevation, V=velocity).

1.2. Iran and hydro power energy

Presently, there are 42 operative hydro power plants with total installed capacity of 7.7 GW and other ones with total capacity of 6.6 GW are also under construction. Out of the operative plants, number of big, medium, small and mini/macro plants are 6, 12, 12 and 12 respectively. The big hydro plants, ranging above 0.1 GW, cover more than 90% of the present installed capacity. Further, it is planned to construct more big and medium hydro units, enhancing the present capacity behind 25 GW [3].

Considering the large number of narrow channels, Iran might be expected to have significant potential for implementing tidal energy schemes. Hence, thousands of small and mini/macro hydro systems can easily be installed through these channels which can provide locally needed electricity or to be fed to local grids. However, studies into the feasibility of implementation of tidal energy in Iran are nevertheless rare at an early stage (Fig. 1).

1.3. Tides around Iran

The tides around Iran are complex, with maximum tidal elevation amplitudes occurring in the Khowr-e Musa Bay. Locations in the south-western part of Iran (NW Persian Gulf) are mostly dominated by semidiurnal tides, whilst those in the south-eastern part of Iran (NW Omman Sea) are dominated by mixed semidiurnal tides [7]. The highest tide in south-western part of Iran is located in the Khowr-e Musa Bay (Fig. 1). In the middle bay current velocities are higher than 2 m/s, the enough value for economic operation of a tidal stream power plant (Fig. 2). Other site that would fulfil the criteria is the Qeshm canal. The largest current magnitudes in the Qeshm canal, on the order of 1.5 m/s, are found along the cross-section between LOFT Jetty and Pt. POHL, where the strait width decreases to a mere 2400 m [5] (Figs. 1 and 3).

This paper is aimed at estimating the practically exploitable tidal energy resource in the Khowr-e Musa Bay. The Khowr-e Musa Bay is a large coastal embayment on the south-western coast of Iran in which the peak tidal currents exceed 2 m/s. It is almost 35.5 km long and leads to a channel about 22.5 km long, which ends at Mahshahr port. The width of the bay varies from 800 m at its narrowest section to 40 km at the mouth, while the depth varies from around 2–3 m in coastal areas to a maximum depth in the mid channel of around 89 m (Fig. 2).

2. Tidal energy resource data

The datasets used for the tide analysis are acquired from the National Cartographic Center of Iran (N.C.C.) and Iran Ports and Maritime Organization (P.M.O.). The Hydrographic Department of N.C.C. collects and distributes observations and predictions of water levels and currents to ensure safe, efficient and environmentally sound maritime commerce. The center manages the national water level observation network in major Iran harbors (http://www.iranhydrography.org). Current data of the current measurement station was reported for the depth of 33.15 m with 5-min interval times (since 6 November 1996 to 7 December 1996), so as to cover the spring–neap variation (Fig. 6).

3. Tidal stream energy conversion methodology

The kinetic energy passing through a vertical cross-section perpendicular to the flow direction per unit time, or in other words the power available from the kinetic energy of the water flowing through the section, is given by [4]

$$P_{KE} = \frac{1}{2}\rho A V^3 \tag{1}$$

where ρ is the water density, A is the surface area of the cross-section, and V is the magnitude of the flow velocity averaged over the section. The tidal stream power density is then given by [4]

$$p_{KE} = \frac{1}{2}\rho V^3 \tag{2}$$

This quantity represents the flow of kinetic energy per square meter of turbine aperture due to the tidal stream. However, not all this power can be converted in practice due to Betz' law and the mechanical losses in the turbines. These limitations related to turbine efficiency are accounted for via the power coefficient (C_P), so that the effective power density, i.e., the power density that the turbine can harness, is [4]

$$p_e = \frac{1}{2}C_p \rho V^3 \tag{3}$$

4. Tidal stream resource methodology

The energy produced in a lunar month for each channel cross-section was estimated by applying the following algorithm:

1. Calculate the water power density at each 5 min increment. The power density can be computed by applying Eq. (2).

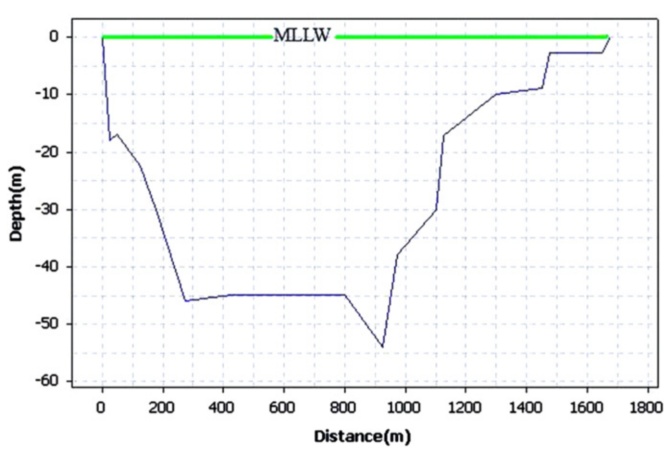


Fig. 4. Channel cross-section area at point A.

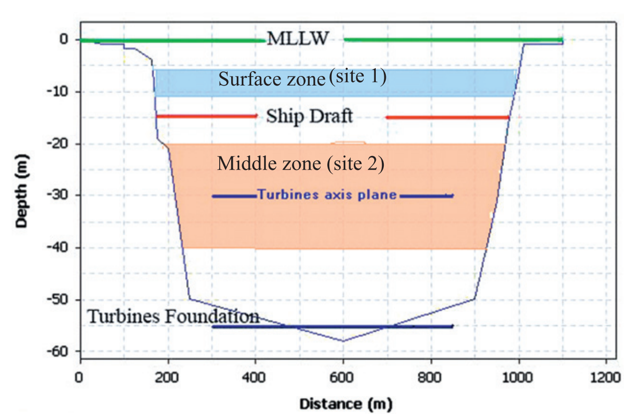


Fig. 5. Channel cross-section area at point B.

2. Calculate the water energy density in each 5 min interval by multiplying the average of the upper and lower bounding power densities by 1/12 hour.

The calculation must then account for the vertical variability of current speed with depth, and its horizontal variability across the channel. This yields an estimate for the mean monthly, depth-averaged, width-averaged tidal stream power density. It was assumed that velocity is constant across the width of the channel.

4.1. Extrapolation of velocity time history to a different channel section

In some cases, current data or predictions may be available in a region outside of a constricted channel where a tidal in-stream energy conversion plant might be sited. This is the case for site in the Khowr-e Musa Bay, where the potential tidal in-stream energy conversion project site is at narrow transect (point B) where the channel flow is most constricted (Figs. 2 and 5) and the tidal currents are fastest, but the tidal current measurement station is at wide transect (point A) where the currents are slower (Figs. 2 and 4).

Assuming the flow does decelerate uniformly and is subcritical (Froude number <1), two open-channel fundamental equations can be applied to make this extrapolation. The first invokes continuity (conservation of mass), and the second invokes conservation of energy. The open-channel energy equation, neglecting the friction loss term, is [7,9]

$$z_1+h_1+\frac{(U_1)^2}{2g}=z_2+h_2+\frac{(U_2)^2}{2g} \tag{4}$$

The continuity of mass equation in terms of channel width and depth is [7]

$$W_1h_1U_1=W_2h_2U_2 \tag{5}$$

z, h, U, g and W are seabed elevation, flow depth, depth-averaged velocity, acceleration due to gravity (9.81 m/s^2) and channel width, respectively.

And re-arranging to state h_2 in terms of U_2:

$$U_2=\frac{W_1h_1U_1}{W_2h_2} \tag{6}$$

and then substituting this expression for h_2 in the energy equation above yields an equation with two real roots, only one of which matches the known flow conditions at narrow transect. The resource analysis method employed here is embedded in a computer program that is prepared for this purpose.

Moon cycles	Date	Time (hh : mm)	Surface velocity (m/s) Point A	Average Velocity (m/s) Point A	Flow Power Density (Kw/m^2)	Flow Power (Kw) Point A	INC of kinetic energy (Kwh) Point A
3rd Qtr Neap tides	1996/11/07	0:00	0.73	0.66	0.15	7106	
	1996/11/07	0:05	0.70	0.63	0.13	6265	557.1
	1996/11/07	0:10	0.67	0.61	0.12	5494	489.9
	1996/11/07	0:15	0.65	0.59	0.11	5016	437.9
	.	.	.	.	.	.	.
	.	.	.	.	.	.	.
	.	.	.	.	.	.	.
New Moon Spring tides	1996/11/12	2:35	1.60	1.45	1.58	74820	.
	1996/11/12	2:40	1.75	1.59	2.06	97897	7196.5
	1996/11/12	2:45	1.80	1.63	2.24	106530	8517.7
	1996/11/12	2:50	1.83	1.66	2.36	111946	9103.1
	.	.	.	.	.	.	.
	.	.	.	.	.	.	.
	.	.	.	.	.	.	.
1st Qtr Neap tides	1996/11/19	21:45	0.97	0.88	0.35	16671	.
	1996/11/19	21:50	0.99	0.90	0.37	17724	1433.1
	1996/11/19	21:55	1.01	0.92	0.40	18820	1522.7
	1996/11/19	22:00	1.02	0.93	0.41	19384	1591.8
	.	.	.	.	.	.	.
	.	.	.	.	.	.	.
	.	.	.	.	.	.	.
Full Moon Spring tides	1996/11/27	23:40	1.90	1.72	2.62	124219	.
	1996/11/27	23:45	1.83	1.66	2.34	111231	9810.4
	1996/11/27	23:50	1.77	1.61	2.13	101125	8848.2
	1996/11/27	23:55	1.70	1.54	1.85	88034	7881.6
	.	.	.	.	.	.	.
	.	.	.	.	.	.	.
	.	.	.	.	.	.	.
3rd Qtr	1996/12/5	3:30	1.55	1.40	1.43	68022	.
	1996/12/5	3:35	1.61	1.46	1.60	76231	6010.5
	1996/12/5	3:40	1.68	1.53	1.82	86613	6785.1
	1996/12/5	3:45	1.65	1.50	1.73	82055	7027.8
Sum of 29 days	8352 recorded data						11496 Mwh/month

Fig. 6. Tidal current energy resource estimation at wide transect (point A).

Moon cycles	Date	Time (hh : mm)	Surface velocity (m/s) Point A	Froude number	Calculated Bernoulli velocity (m/s) for Point B	Calculated depth (m) Point B	Surface velocity (m/s) point B	Surface actual velocity (m/s) Point B
3rd Qtr Neap tides	1996/11/07	0:00	0.73	0.031	1.080	39.98	1.11	0.92
	1996/11/07	0:05	0.70	0.030	1.040	39.96	1.07	0.89
	1996/11/07	0:10	0.67	0.029	0.995	39.98	1.03	0.86
	1996/11/07	0:15	0.65	0.028	0.965	41.22	0.99	0.82
	...	...	...	...	...	...	...	...
New Moon Spring tides	1996/11/12	2:35	1.60	0.069	2.383	39.87	2.46	2.04
	1996/11/12	2:40	1.75	0.075	2.608	39.85	2.69	2.23
	1996/11/12	2:45	1.80	0.077	2.684	39.82	2.77	2.30
	1996/11/12	2:50	1.83	0.079	2.729	39.81	2.82	2.34
	...	...	...	...	...	...	...	...
1st Qtr Neap tides	1996/11/19	21:45	0.97	0.0419	1.441	39.97	1.48	1.23
	1996/11/19	21:50	0.99	0.0428	1.471	39.96	1.52	1.26
	1996/11/19	21:55	1.01	0.0437	1.501	39.95	1.55	1.29
	1996/11/19	22:00	1.02	0.0441	1.516	39.95	1.56	1.30
	...	...	...	...	...	...	...	...
Full Moon	1996/11/27	23:40	1.90	0.090	2.834	39.81	2.92	2.42
	1996/11/27	23:45	1.83	0.087	2.729	39.82	2.82	2.34
	1996/11/27	23:50	1.77	0.084	2.639	39.82	2.72	2.26
	1996/11/27	23:55	1.70	0.080	2.533	39.85	2.61	2.17
	...	...	...	...	...	...	...	...
3rd Qtr	1996/12/5	3:30	1.55	0.067	2.308	39.88	2.38	1.98
	1996/12/5	3:35	1.61	0.069	2.398	39.86	2.47	2.05
	1996/12/5	3:40	1.68	0.072	2.503	39.85	2.58	2.14
	1996/12/5	3:45	1.65	0.071	2.458	39.86	2.54	2.11

Fig. 7. Tidal current estimation at narrow transect (point B).

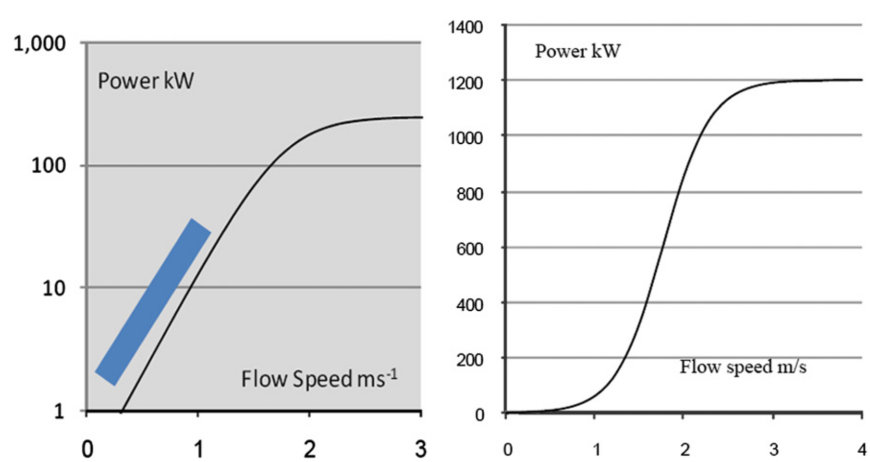


Fig. 8. Neptune NP1000 power curve (left), Marine Current Turbine SeaGen simulated power curve (right) [8].

4.2. Quantification of the tidal stream resource

In this work, solving the conservation of energy equation coupled with the continuity of mass equation allows us to estimate the velocity magnitude (V) at point B (Fig. 7). Since Bernoulli's theoretical current velocity does not account for the channel dimensions and bathymetry; this can be used to estimate the actual current velocity of the channel by applying channel loss correction factor K_L (Fig. 7). The depth-averaged velocity magnitude at both transects is shown in Figs. 6 and 9 during a 29-day period, so as to cover the spring–neap variation. Peak values in spring are 1.72 and 2.24 m/s at points A and B, respectively.

Moon cycles	Date	Time (hh : mm)	Surface actual velocity (m/s) point B	Hub actual velocity (m/s) point B	Average Actual Velocity (m/s) Point B	Flow Power Density (Kw/m^2)	Flow Power (Kw) Point B	INC of energy (Kwh) Point B
3rd Qtr Neap tides	1996/11/07	0:00	0.92	0.86	0.84	0.30	11783	.
	1996/11/07	0:05	0.89	0.82	0.81	0.27	10438	1851
	1996/11/07	0:10	0.86	0.79	0.78	0.24	9499	1661
	1996/11/07	0:15	0.82	0.76	0.75	0.21	8337	1486
	.	.	.	.	.	.	.	.
New Moon Spring tides	1996/11/12	2:35	2.04	1.89	1.86	3.30	128537	.
	1996/11/12	2:40	2.23	2.07	2.03	4.31	168183	24726
	1996/11/12	2:45	2.30	2.13	2.09	4.69	183014	29266
	1996/11/12	2:50	2.34	2.16	2.13	4.92	191868	31240
	.	.	.	.	.	.	.	.
1st Qtr Neap tides	1996/11/19	21:45	1.23	1.14	1.12	0.72	28137	.
	1996/11/19	21:50	1.26	1.16	1.15	0.77	30055	4849
	1996/11/19	21:55	1.29	1.19	1.17	0.82	32058	4515
	1996/11/19	22:00	1.30	1.20	1.18	0.84	32745	5176
	.	.	.	.	.	.	.	.
Full Moon	1996/11/27	23:40	2.42	2.24	2.21	5.52	215242	.
	1996/11/27	23:45	2.34	2.16	2.13	4.92	191868	33925
	1996/11/27	23:50	2.26	2.15	2.06	4.47	174437	30525
	1996/11/27	23:55	2.17	2.00	1.98	3.95	154175	27384
	.	.	.	.	.	.	.	.
3rd Qtr	1996/12/5	3:30	1.98	1.83	1.80	3.00	116859	.
	1996/12/5	3:35	2.05	1.89	1.87	3.34	130266	20593
	1996/12/5	3:40	2.14	1.98	1.95	3.81	148418	23223
	1996/12/5	3:45	2.11	1.94	1.92	3.61	140967	24115
Sum of 29days								20052Mwh

Fig. 9. Tidal current energy resource estimation at narrow transect (point B).

The highest velocities within each semidiurnal cycle occur during the spring tides, as indicated.

The time distribution of the power density at both points is shown in Figs. 6 and 9. The difference in peak velocity between them is again amplified by the cubic exponent, resulting in a large disparity in power density values: 2.62 kW/m^2 and 5.52 kW/m^2 at points A and B, respectively. For the same reason, the peak values during the spring are much larger than those during the neap. The maxima at neap are 1.43 and 3 kW/m^2 at points A and B respectively. The estimation of kinetic energy at both points is shown in Figs. 6 and 9 during a 29-day period. By summing up the two tables, the total available tidal stream resource was derived. The total available tidal stream resource would be 11 496 MW h/month and 20 052 MW h/month at points A and B, respectively.

The total power in the flow at a site cannot be extracted for energy production. The extractable energy is limited by channel geometry and environmental considerations. For typical commercial-scale tidal projects at most sites, the 15% environmental extraction constraint will be the limiting factor [6,7]. The channel extractable resource was calculated by applying this environmental limiting factor. The channel extractable resource would be 3008 MW h/month at narrow transect (point B).

5. Tidal stream power production methodology

In order to characterize with more precision the tidal stream resource in the bay narrow transect, two sites are selected: site 1 in the zone with the highest power density and site 2 in the zone with a somewhat lower power density, but more separated from the navigational clearance zone (Fig. 5). The installation of a tidal stream power plant at site 1 would require a delimitation of the navigation channel leading to the Mahshahr port.

In the first selected site, the relationship between cut-in speed and rated speed was taken from the Neptune Renewable Energy Ltd NP1000 vertical-axis tidal turbine, which was reported to have a cut in speed of 0.5 m/s and achieved rated power at around 3 m/s [8,9]. In the second selected site, the relationship between

Moon cycles	Date	Time (hh : mm)	Surface actual velocity (m/s) point S	incoming flow-V_∞ Applying Cosine factor(m/s)	incoming flow power (Kw)	incoming flow INC of energy (Kwh)	NP1000 Power (Kw)	NP1000 Out put INC of energy (Kwh)
3rd Qtr Neap tides	1996/11/07	0:00	0.92	0.918	33		10.5	
	1996/11/07	0:05	0.89	0.885	30	2.6	10.5	0.9
	1996/11/07	0:10	0.86	0.852	26	2.3	10.5	0.9
	1996/11/07	0:15	0.82	0.819	23	2.0	8.50	0.8
	.	.	.	.	.	.	.	.
	.	.	.	.	.	.	.	.
	.	.	.	.	.	.	.	.
New Moon Spring tides	1996/11/12	2:35	2.04	2.035	359	.	172	.
	1996/11/12	2:40	2.23	2.225	469	34.5	196	15.3
	1996/11/12	2:45	2.30	2.292	513	40.9	210	16.9
	1996/11/12	2:50	2.34	2.333	541	43.9	210	17.5
	.	.	.	.	.	.	.	.
	.	.	.	.	.	.	.	.
	.	.	.	.	.	.	.	.
1st Qtr Neap tides	1996/11/19	21:45	1.23	1.224	78	.	30	.
	1996/11/19	21:50	1.26	1.257	85	6.8	47	3.2
	1996/11/19	21:55	1.29	1.282	90	7.3	47	3.9
	1996/11/19	22:00	1.30	1.291	92	7.6	47	3.9
	.	.	.	.	.	.	.	.
	.	.	.	.	.	.	.	.
	.	.	.	.	.	.	.	.
Full Moon	1996/11/27	23:40	2.42	2.416	601	.	223	.
	1996/11/27	23:45	2.34	2.333	541	47.6	210	18.0
	1996/11/27	23:50	2.26	2.250	485	42.8	210	17.5
	1996/11/27	23:55	2.17	2.159	429	38.1	196	16.9
	.	.	.	.	.	.	.	.
	.	.	.	.	.	.	.	.
	.	.	.	.	.	.	.	.
3rd Qtr	1996/12/5	3:30	1.98	1.969	325	.	172	.
	1996/12/5	3:35	2.05	2.043	363	28.7	172	14.3
	1996/12/5	3:40	2.14	2.134	414	32.4	179	14.6
	1996/12/5	3:45	2.11	2.101	395	33.7	179	14.9
Sum of 29 days						41.84Mwh		17.8Mwh

Fig. 10. The monthly output energy (kW h) by one Neptune Proteus NP1000 device.

cut-in speed and rated speed was taken from the Marine Current Turbines Ltd SeaGen horizontal-axis turbine, which was reported to have a cut-in speed of 0.7 m/s and achieved rated power at around 3 m/s [9,10]. This study examines the possible power recoverable for these devices, based on their published power curves (Fig. 8) [8].

By applying the device power curve (Fig. 8) the electrical power output was calculated. The electrical energy output (E_{out}) was calculated by multiplying the average of the upper and lower bounding powers by 1/12 hour. By summing up the two tables, the monthly output (MW h/month) per device was derived. The scatter diagram for the monthly energy is shown in Fig. 10, related to Neptune NP1000 device, and the scatter diagram for the monthly energy is shown in Fig. 11 related to MCT SeaGen device.

Water to wire efficiency was calculated by dividing the free flow energy available for standard lunar month cycle (E_{in}) by the turbine output energy for standard lunar month cycle (E_{out}) [10] (Figs. 10 and 11). The water-to-wire efficiency equals to 42.54% and 33.48% for Neptune Proteus NP1000 and MCT SeaGen device, respectively. It is important to note that the water-to-wire efficiencies may not be representative of the optimum efficiency for lowest cost of electricity produced; that is, a lower efficiency with a simpler energy conversion machine may produce a lower cost of electricity system than a higher efficiency conversion device [10].

5.1. Optimal number of turbines

The number of turbines could be gauged by observing the loss of energy which resulted from the reduction of the current velocity in the channel. It is possible to estimate the decay in flow speed for a large-scale array using momentum theory. From this theory the relationship between the free stream velocity and that just downstream of the rotor is given by [11]

$$V_e = (1-2a)V_\infty \quad (7)$$

where V_e is the wake velocity and V_∞ the inflow velocity. a is the rotor axial induction factor so that $a=1/3$ when the rotor is operating at maximum efficiency thus we can assume that $V_e = U_0/3$. This is the efficiency with which the turbine extracts kinetic energy from the incoming flow [11]. An estimate of the average operating axial induction factor was taken as 1/4

Moon cycles	Date	Time (hh : mm)	Hub actual velocity (m/s) point H	incoming flow-V_∞ Applying Cosine factor(m/s)	incoming flow power (Kw)	incoming flow INC of energy (Kwh)	MCT Power (Kw)	MCT Out put INC of energy (Kwh)
3rd Qtr Neap tides	1996/11/07	0:00	0.86	0.857	190		72	
	1996/11/07	0:05	0.82	0.817	165	14.8	51	5.1
	1996/11/07	0:10	0.79	0.787	147	13.0	51	4.3
	1996/11/07	0:15	0.76	0.757	131	11.6	51	4.3
	.	.	.	.	.	.	.	.
New Moon Spring tides	1996/11/12	2:35	1.89	1.883	2017	.	698	.
	1996/11/12	2:40	2.07	2.062	2648	194.4	876	65.6
	1996/11/12	2:45	2.13	2.122	2886	230.6	876	73.0
	1996/11/12	2:50	2.16	2.152	3011	245.7	997	78.0
	.	.	.	.	.	.	.	.
1st Qtr Neap tides	1996/11/19	21:45	1.14	1.136	443	.	126	.
	1996/11/19	21:50	1.16	1.156	467	37.9	164	12.1
	1996/11/19	21:55	1.19	1.185	503	40.4	164	13.7
	1996/11/19	22:00	1.20	1.195	515	42.4	164	13.7
	.	.	.	.	.	.	.	.
Full Moon	1996/11/27	23:40	2.24	2.231	3354	.	997	.
	1996/11/27	23:45	2.16	2.152	3011	265.2	997	83.1
	1996/11/27	23:50	2.15	2.142	2969	249.1	876	78.0
	1996/11/27	23:55	2.00	1.992	2388	223.2	814	70.4
	.	.	.	.	.	.	.	.
3rd Qtr	1996/12/5	3:30	1.83	1.820	1821	.	624	.
	1996/12/5	3:35	1.89	1.886	2027	160.3	690	54.6
	1996/12/5	3:40	1.98	1.969	2306	180.5	810	62.5
	1996/12/5	3:45	1.94	1.936	2192	187.4	698	62.8
Sum of 29 days						222.8Mwh		74.6Mwh

Fig. 11. The monthly output energy (kW h) by one MCT SeaGen device.

meaning that $V_e = U_\infty/2$ and thus the wake velocity deficit immediately downstream of the rotor is 0.5.

The magnitudes of decelerating flow are shown in Figs. 12 and 13. By summing up the two tables, the monthly captured energy (MW h/month) per device was derived. The scatter diagram for the monthly energy is shown in Fig. 12, related to Neptune NP1000 device, and the scatter diagram for the monthly energy is shown in Fig. 13 related to MCT SeaGen device. Applying this result for the loss of energy associated with the channel extractable resource, it is possible to investigate the optimum number of turbines by considering conservation of energy. The optimum number of turbines equals to 96 and 17 at sites 1 and 2, respectively.

5.2. Turbine distribution in the farm

Besides tidal flow velocity, the two most important control variables for energy cost are turbine relative distance and farm size [12]. For turbines with constructive hydrodynamic interaction the power output of the turbines with optimal design can be more than that of the turbines which are located far away from each others, i.e., there is no hydrodynamic interaction between turbines [12]. In general, the optimal tandem distance is 6–10 times turbine diameter for vertical axis turbines [13] and three times turbine diameter for horizontal axis turbines [14]. The energy cost also reduces when the farm scale becomes larger as the operational and maintenance cost per turbine reduces [13]. Further study could be conducted to find the most optimal tidal array configuration.

6. Compatibility and impacts on recreation and tourism

The most important potential influence of floating tidal energy conversion devices on recreation and tourism is due to visual impact, which is likely to prove an important obstacle to large-scale deployment of floating tidal energy schemes in areas of tourism or aesthetic importance. Killer whale-like cover or other appropriate cover are solution for these problems [15].

7. Conclusions

Iran has an excellent hydro power energy resource and the use of this resource will assist in the development of a sustainable energy future. Iran – with its many narrow channels and significant tidal range – might be expected to have considerable potential for tidal current power generation. The Khowr-e Musa Bay is a large

Moon cycles	Date	Time (hh : mm)	Surface actual velocity (m/s) point B	incoming flow-V_∞ Applying Cosine factor(m/s)	incoming flow power (Kw)	incoming flow INC of energy (Kwh)	Outgoing flow-v_e (m/s)	Outgoing flow power Applying K_T	Outgoing flow INC of energy (Kwh)
3rd Qtr Neap tides	1996/11/07	0:00	0.92	0.918	33	2.6	0.46	4.1	
	1996/11/07	0:05	0.89	0.885	30	2.3	0.44	3.7	0.33
	1996/11/07	0:10	0.86	0.852	26	2.0	0.43	3.3	0.29
	1996/11/07	0:15	0.82	0.819	23	.	0.41	2.9	0.26
	.	.	.	.	.	.	.	.	.
	.	.	.	.	.	.	.	.	.
New Moon Spring tides	1996/11/12	2:35	2.04	2.035	359	34.5	1.02	44.9	.
	1996/11/12	2:40	2.23	2.225	469	40.9	1.11	58.7	4.31
	1996/11/12	2:45	2.30	2.292	513	43.9	1.15	64.1	5.12
	1996/11/12	2:50	2.34	2.333	541	.	1.17	67.6	5.49
	.	.	.	.	.	.	.	.	.
	.	.	.	.	.	.	.	.	.
1st Qtr Neap tides	1996/11/19	21:45	1.23	1.224	78	6.8	0.61	9.8	.
	1996/11/19	21:50	1.26	1.257	85	7.3	0.63	10.6	0.85
	1996/11/19	21:55	1.29	1.282	90	7.6	0.64	11.2	0.91
	1996/11/19	22:00	1.30	1.291	92	.	0.65	11.5	0.94
	.	.	.	.	.	.	.	.	.
	.	.	.	.	.	.	.	.	.
Full Moon	1996/11/27	23:40	2.42	2.416	601	47.6	1.21	75.1	.
	1996/11/27	23:45	2.34	2.333	541	42.8	1.17	67.6	5.95
	1996/11/27	23:50	2.26	2.250	485	38.1	1.13	60.7	5.34
	1996/11/27	23:55	2.17	2.159	429	2.6	1.08	53.6	4.76
	.	.	.	.	.	.	.	.	.
	.	.	.	.	.	.	.	.	.
3rd Qtr	1996/12/5	3:30	1.98	1.969	325	.	0.98	40.6	.
	1996/12/5	3:35	2.05	2.043	363	28.7	1.02	45.4	3.59
	1996/12/5	3:40	2.14	2.134	414	32.4	1.07	51.7	4.05
	1996/12/5	3:45	2.11	2.101	395	33.7	1.05	49.4	4.21
Sum of 29days						41.84Mwh Captured energy 36.61Mwh			5.23 Mwh

Fig. 12. The monthly captured energy (kW h) by one Neptune Proteus NP1000 device.

coastal embayment on the south-western coast of Iran in which the peak tidal currents exceed 2 m/s. Should be recognized as a technical potential and presents a possible scheme for a large-scale roll-out, whereas the result from the present work is more to be considered as gross tidal in-stream energy potential for two site in the Khowr-e Musa Bay. The case shown here illustrates two devices and devices were chosen mainly based on the power flux in the tidal currents. Thorough economical analysis is required prior to any real installation plans. With the aim of quantifying the tidal stream resource and assessing the viability of a tidal stream plant, a statistical method has been implemented. Four significant conclusions emerge from the calculation of output power from arrays of two of the devices:

1. The highest tidal velocities were seen to occur in the bay narrow transect (point B), with maxima around 2.24 m/s at mid-flood of a spring tide. At mid-flood of a mean spring tide the power density, or power per square meter of turbine aperture, reaches a maximum of 5.52 kW/m^2 at point B. The total available tidal stream resource would be 11 496 MW h/month and 20 052 MW h/month at points A and B, respectively. The total available resource is two times greater in the constriction than in the wide channel. The maximum extractable tidal stream energy resource would be 3008 MW h/month at narrow transect.
2. Two sites were chosen for closer examination, both in the bay narrow transect (point B). Site 1 is close to the surface zone, and site 2, to the middle zone. We studied power recoverable possibility for two different tidal in stream conversion devices, based on their published power curves; Neptune Proteus NP1000 device at site 1 and Marine Current Turbine SeaGen device at site 2. For Neptune Proteus NP1000 device, average electric power generation would be 17.8 MW h/month and for MCT SeaGen device, average electric power generation would be 74.6 MW h/month. The water-to-wire efficiency of the Neptune Proteus NP1000 device would be 42.54% and the water-to-wire efficiency of the MCT SeaGen device would be 33.48%. When deciding upon the optimum location of a tidal stream power plant in the Khowr-e Musa Bay, the advantage of the higher energy output at the first site must be weighed against its relative proximity to the second location. Should the plant be installed at site 1, a clear delimitation of the navigational channel would be essential.
3. Two different farm sizes were identified: large scale (96 turbines) at site 1 and small scale (17 turbines) at site 2. Further study could be conducted to find the most optimal tidal array configuration.
4. The killer whale-like cover is proposed for floating tidal energy conversion devices. Killer whale-like cover and other appropriate cover create a beautiful view and compatibility with environment.

Moon cycles	Date	Time (hh : mm)	Hub actual velocity (m/s) point B	incoming flow-V_∞ Applying Cosine factor(m/s)	incoming flow power (Kw)	incoming flow INC of energy (Kwh)	Outgoing flow-v_e (m/s)	Outgoing flow power Applying K_T	Outgoing flow INC of energy (Kwh)
3rd Qtr Neap tides	1996/11/07	0:00	0.86	0.857	190		0.428	24	
	1996/11/07	0:05	0.82	0.817	165	14.8	0.408	21	1.8
	1996/11/07	0:10	0.79	0.787	147	13.0	0.394	18	1.6
	1996/11/07	0:15	0.76	0.757	131	11.6	0.379	16	1.4
	.	.	.	.	.	.	.	.	.
	.	.	.	.	.	.	.	.	.
New Moon Spring tides	1996/11/12	2:35	1.89	1.883	2017	.	0.942	252	.
	1996/11/12	2:40	2.07	2.062	2648	194.4	1.031	331	24.3
	1996/11/12	2:45	2.13	2.122	2886	230.6	1.061	361	28.8
	1996/11/12	2:50	2.16	2.152	3011	245.7	1.076	376	30.7
	.	.	.	.	.	.	.	.	.
	.	.	.	.	.	.	.	.	.
1st Qtr Neap tides	1996/11/19	21:45	1.14	1.136	443	.	0.568	55	.
	1996/11/19	21:50	1.16	1.156	467	37.9	0.578	58	4.7
	1996/11/19	21:55	1.19	1.185	503	40.4	0.593	63	5.0
	1996/11/19	22:00	1.20	1.195	515	42.4	0.598	64	5.3
	.	.	.	.	.	.	.	.	.
	.	.	.	.	.	.	.	.	.
Full Moon	1996/11/27	23:40	2.24	2.231	3354	.	1.115	419	.
	1996/11/27	23:45	2.16	2.152	3011	265.2	1.076	376	33.2
	1996/11/27	23:50	2.15	2.142	2969	249.1	1.071	371	31.1
	1996/11/27	23:55	2.00	1.992	2388	223.2	0.996	298	27.9
	.	.	.	.	.	.	.	.	.
	.	.	.	.	.	.	.	.	.
3rd Qtr	1996/12/5	3:30	1.83	1.820	1821	.	0.910	228	.
	1996/12/5	3:35	1.89	1.886	2027	160.3	0.943	253	20.0
	1996/12/5	3:40	1.98	1.969	2306	180.5	0.984	288	22.5
	1996/12/5	3:45	1.94	1.936	2192	187.4	0.968	274	23.4
Sum of 29 days						222.8Mwh Captured energy 195Mwh			27.8 Mwh

Fig. 13. The monthly captured energy (kW h) by one MCT SeaGen device.

Acknowledgments

The author is grateful to the anonymous reviewers for their valuable comments, and to Dr. A.H. Javid, for the numerical and graphical computer work related to (Fig. 2) and to Dr. S. Hasanzadeh.

References

[1] Mohammadnejad M, Ghazvini M, Mahlia TMI, Andriyana A. A review on energy scenario and sustainable energy in Iran. Renewable and Sustainable Energy Reviews 2011;15:4652–8.
[2] Google earth maps; 2009 〈http://earth.google.com〉.
[3] Ghorashi AH, Rahimi AH. Renewable and non-renewable energy status in Iran: art of know-how and technology-gaps, Renewable and Sustainable Energy Reviews 2011;15:729–36.
[4] Carballo R, Iglesias G, Castro A. Numerical model evaluation of tidal stream energy resources in the Ria de Muros (NW Spain). Renewable Energy 2009;34:1517–24.
[5] Abbaspour M, Rahimi R. Iran atlas of offshore renewable energies. Renewable Energy 2011;36:388–98.
[6] Bryden IG, Grinsted T, Melville GT. Assessing the potential of a simple tidal channel to deliver useful energy. Applied Ocean Research 2004;26:198–204.
[7] Hagerman G, Polagye B. EPRI-TP-001 NA Rev 3; 2006 〈http://www.epri.com/oceanenergy〉.
[8] Hardisty J. The tidal stream power curve: a case study, Energy and Power Engineering 2012;4:132–6.
[9] Hardisty J. The analysis of tidal stream power. Chichester: Wiley; 2009.
[10] Bedard R. Survey and characterisation of tidal in stream energy conversion (TISEC) devices. Report EPRI TP 004 NA; 2005 〈http://www.epri.com/oceanenergy〉.
[11] Myers L, Bahaj AS. Simulated electrical power potential harnessed by marine current turbine arrays in the Alderney Race. Renewable Energy 2005;30:1713–31.
[12] Li Y, Lence Barbara J, Calisal Sander M. An integrated model for estimating energy cost of a tidal current turbine farm. Energy Conversion and Management 2011;52:1677–87.
[13] Li Y, Lence Barbara J, Calisal Sander M. Modeling the energy output from an in-stream tidal turbine farm. Journal of Computers 2009;4:288–94.
[14] Ho Lee S, Hyuk Lee S, Jang K, Lee J, Hur N. A numerical study for the optimal arrangement of ocean current turbine generators in the ocean current power parks. Current Applied Physics 2010;10:137–41.
[15] Rashid A, Hasanzadeh S. Status and potentials of offshore wave energy resources in Chahbahar area (NW Omman Sea). Renewable and Sustainable Energy Reviews 2011;15:4876–83.